Well-Differentiated Papillary Mesothelioma of the Peritoneum is Genetically Distinct from Malignant Mesothelioma

Raunak Shrestha[1,2], Noushin Nabavi[1,3], Stanislav Volik[1], Shawn Anderson[1], Anne Haegert[1], Brian McConeghy[1], Sonal Brahmbhatt[1], Robert H. Bell[1], Stephane Le Bihan[1], Yuzhuo Wang[2,3], Colin C. Collins[1,2,*], and Andrew Churg[4,*]

[1]Vancouver Prostate Centre, Vancouver, BC, Canada

[2]Department of Urologic Sciences, University of British Columbia, Vancouver, BC, Canada

[3]Department of Experimental Therapeutics, BC Cancer Agency, Vancouver, BC, Canada

[4]Department of Pathology, Vancouver General Hospital, Vancouver, BC, Canada

[*]Correspondence should be addressed to Andrew Churg, MD, Department of Pathology, Vancouver General Hospital, 910 W 10th Ave, Vancouver, BC, V5Z 1M9, Canada (achurg@mail.ubc.ca), and Collin C. Collins, PhD, Vancouver Prostate Centre, 2660 Oak Street, Vancouver, BC, V6H 3Z6, Canada (ccollins@prostatecentre.com)

Running Title: Molecular characterization of WDPM

Keywords: Well-differentiated papillary mesothelioma, DNA sequencing, mutation

Abstract

Well-differentiated papillary mesothelioma (WDPM) is an uncommon mesothelial proliferation that is most commonly encountered as an incidental finding in the peritoneal cavity. There is controversy in the literature about whether WDPM is a neoplasm or a reactive process, and if neoplastic, whether it is a variant or precursor of epithelial malignant mesothelioma or is a different entity. Using whole exome sequencing of five WDPM of the peritoneum, we have identified distinct mutations in *EHD1*, *ATM*, *FBXO10*, *SH2D2A*, *CDH5*, *MAGED1*, and *TP73* shared by WDPM cases but not reported in malignant mesotheliomas. Furthermore, we show that WDPM is strongly enriched with C>A transversion substitution mutations, a pattern that is also not found in malignant mesotheliomas. The WDPMs lacked alterations involving *BAP1*, *SETD2*, *NF2*, *CDKN2A/B*, *LASTS1/2*, *PBRM1* and *SMARCC1* that are frequently altered in malignant mesotheliomas. We conclude that WDPMs are genetically distinct from malignant mesotheliomas, and based on observed mutations do not appear to be precursors of malignant mesotheliomas.

Introduction

Well-differentiated papillary mesothelioma (WDPM) is a morphologically distinctive papillary proliferation of mesothelial cells that is most commonly encountered as an incidental finding in the peritoneal cavity, and less often in the pleural cavity, pericardium, and tunica vaginalis. These lesions may be single or multiple, but by definition do not invade the underlying stroma and usually behave in a benign or indolent fashion, sometimes persisting for many years[1]. However, the nature of WDPM is disputed, with theories ranging from a reactive non-neoplastic process to a benign tumor, to a variant and/or precursor of epithelial malignant mesotheliomas[2]. To add further confusion, unequivocal invasive malignant mesotheliomas can have areas that mimic WDPM. Since malignant mesotheliomas are aggressive tumors, the distinction from WDPM is important, but WDPM are sometimes treated with debulking cytoreductive surgery followed by hyperthermic intraperitoneal chemotherapy (HIPEC) as if they were mesotheliomas[3].

Genome-wide sequencing analyses of malignant mesotheliomas have revealed frequently observed genomic aberrations such as loss of function mutation and/or copy number alterations/deletion of *BAP1*, *SETD2*, *CDKN2A*, and *NF2*[4–6]. Studies analyzing WDPM using DNA sequencing technology are limited. Case studies have reported WDPMs with somatic mutation of *E2F1*[7], heterozygous loss of *NF2*[8], and germline *BAP1* mutation[9], which if correct would suggest that they may be variants of malignant mesothelioma. Nevertheless, using immunohistochemistry (IHC) and Fluorescence in situ hybridization (FISH), Lee *et al.* demonstrated that, unlike in malignant mesothelioma, both *BAP1* and *CDKN2A* are intact and respective proteins are expressed in WDPMs[10]. More recently, Stevers *et al.*[11] performed genomic profiling of 10 WDPM and found that they harboured *TRAF7* or *CDC42* mutually exclusive missense mutations.

To shed further light on this question we performed an extensive genomic characterization of a cohort of five WDPMs of the peritoneum.

Materials and methods

Patient cohort description and tissue procurement

A cohort of incidentally identified WDPM tissues (n=5) were assembled from the surgical pathology archives at the Vancouver General Hospital. This study was approved by the Institutional Review Board of the University of British Columbia and the Vancouver Coastal Health (REB No. H15-00902 and V15-00902).

Whole exome sequencing

DNA from marked Formalin-fixed and paraffin embedded (FFPE) tissue sections (5-10 µm in thickness, ~ 50% WDPM cellularity) were isolated using truXTRAC FFPE DNA Kit with the Covaris' Adaptive Focused Acoustics®(AFA®) technology, which enables the removal of the paraffin from the FFPE tissue in SDS buffer, while simultaneously rehydrating the tissue. The samples were treated with proteinase K 0.2 mg/mL (Roche) followed by overnight incubation at 55°C. After post-incubation in proteinase K, the samples were treated with RNAse and DNA extracted as per the truXTRAC FFPE DNA extraction protocol (Covaris cat#: 520136). The amount of DNA was quantified using the Qubit® dsDNA HS Assay (Thermo Fisher Scientific).

For Ion AmpliSeq™ (Thermo Fisher Scientific) Exome Sequencing, 100ng of DNA was used as input for Ion AmpliSeq™ Exome RDY library preparation, a PCR-based sequencing approach using 294,000 primer pairs (amplicon size range 225-275 bp), which covers >97% of CCDS (Release 12), >19,000 coding genes and >198,000 coding exons. Libraries were prepared, quantified by qPCR and sequenced according to the manufacturer's instructions (Thermo Fisher Scientific). Samples were sequenced on the Ion Proton System using the Ion PI™ Hi□Q™ Sequencing 200 Kit and Ion PI™ v3 chip. Two libraries were run per chip for a projected minimum coverage of 40M reads/sample.

Single nucleotide variant calling

We used Torrent Server (Thermo Fisher Scientific) for mapping aligned reads to the human reference genome hg19 (Torrent Mapping Alignment feature). Variants were identified by Torrent Variant Caller plugin with the optimized parameters for AmpliSeq exome-sequencing (Thermo Fisher Scientific). The variant call format (VCF) files from all sample were annotated using ANNOVAR[12].

To account for the low tumor cellularity in the WDPM samples and the absence of the matched control samples, we used strict mutation calls filtering criteria. Mutations were retained if (a) allele frequency

(AF) < 50%, (b) read quality pass > 50%, (c) average heterozygosity < 0.1, (d) mutation calls present in dbSNP database. We filtered out all In-Dels from our variant calls. Non-silent exonic variants including non-synonymous single nucleotide variations (SNVs), stop-codon gain SNVs, stop-codon loss SNVs, splice site SNVs, and frameshift In-Dels in coding regions were retained if they were supported by more than 50 reads. Furthermore, putative variants were manually scrutinized on the Binary Alignment Map (BAM) files through Integrative Genomics Viewer (IGV) version 2.3.25[13]. Furthermore, due to lack of matched germline control samples from the WDPM cases, we used genomic DNA samples from blood of a cohort of peritoneal mesothelioma patients as germline control samples. We filtered out any variants that were also present in these control samples[6]. In this way, we excluded any potential germline variants as well as false positive calls and obtained highly confident variants of WDPM. Based on the variant allele frequency (VAF), the somatic mutations identified in WDPM were clustered into different groups using the R-package Maftools[14].

Copy number aberration (CNA) calls

Copy number changes were assessed using Nexus Copy Number Discovery Edition Version 8.0 (BioDiscovery, Inc., El Segundo, CA). Nexus NGS functionality with the FASST2 Segmentation algorithm was used to make copy number calls (a Circular Binary Segmentation/Hidden Markov Model approach). The significance threshold for segmentation was $5x10^{-6}$ with a minimum of 3 probes per segment and a maximum probe spacing of 1000 between adjacent probes before breaking a segment. The log ratio thresholds for single copy gain and single copy loss were set at +0.2 and −0.2, respectively. The log ratio thresholds for homozygous gain/loss were set at +0.6 and −1.0, respectively. The tumor BAM files were processed and compared with BAM files from normal tissue pool as reference control. Reference reads per CN point (window size) was set to 8000. We used the Genomic Identification of Significant Targets in Cancer (GISTIC)[15] algorithm in Nexus to identify significantly amplified or deleted regions across the genome. The amplitude of each aberration is assigned a G-score as well as a frequency of occurrence for multiple samples. False Discovery Rate (FDR) q-values for the aberrant regions was set to a threshold of 0.15.

Mutational signature analysis

We used deconstructSigs[16] software, a multiple regression approach to statistically quantify the contribution of mutational signatures for each tumor. The 30 mutational signatures were obtained from the COSMIC mutational signature database[17] (https://cancer.sanger.ac.uk/cosmic/signatures). Only non-

silent somatic mutations were used to obtain the mutational signatures. In brief, deconstructSigs attempts to recreate the mutational pattern using the trinucleotide mutation context from the input sample that closely resembles each of the 30 mutational signatures from COSMIC mutational signature database. In this process, each mutational signature is assigned a weight normalized between 0 to 1 indicating its contribution. Only those mutational signatures with a weight more than 0.06 were considered for analysis.

Pathway enrichment analysis

The mutated genes were tested for enrichment against signaling pathways present in KEGG[18] pathway database obtained from the Molecular Signature Database (MSigDB) v6.0[19]. A hypergeometric test based gene set enrichment analysis was used for this purpose (https://github.com/raunakms/GSEAFisher). A cut-off threshold of Benjamini–Hochberg (BH) corrected *p*-value < 0.01 was used to obtain the significantly enriched pathways. Only pathways that are enriched with at least three mutated genes were considered for further analysis.

Peritoneal mesothelioma datasets

We utilized DNA sequencing datasets of two publicly available patient cohorts of peritoneal mesothelioma - VPC cohort[6] and AACR Project GENIE Cohort[20]. We used mutation and copy number profiles from both datasets for comparison with the genomic profiles of WDPM cases. AACR GENIE Project Data: Version 5.0 was downloaded from https://www.synapse.org/#!Synapse:syn7222066.

Results

Histopathological features of WDPM

All five WDPM cases were incidental findings in the peritoneum detected during surgery for another process and all were solitary lesions. All of these five cases had the typical features described for WDPM[21]; i.e. a papillary architecture with a single layer of covering bland mesothelial cells and myxoid cores in the papillae (**Fig. 1**).

Mutational landscape of WDPM

We performed high-coverage whole exome sequencing of five WDPMs from FFPE samples. We achieved a mean sequencing reads coverage of 87x-117x, with at least 20-45% of targeted bases having a coverage of 100x (**Supplementary Table 1).** Due to papillary architecture, the tumor cellularity of the WDPM tissues were estimated to be about 50% (**Supplementary Table 2)**. Although, the high coverage sequencing provides us an opportunity to detect higher proportions of mutations, the normal tissue admixture lowers the mutation detection sensitivity. To overcome this challenge, we implemented strict mutation filtering criteria as described in the Methods section and retained only high confident mutation calls for downstream analysis.

Analysis of the mutational patterns in WDPM revealed a strong enrichment of C>A transversion substitution mutation (**Fig. 2A**). Using the software deconstructSigs[16], we evaluated the characteristic mutation patterns in WDPM against the mutational signature obtained from the COSMIC mutational signature database[17]. Intriguingly, we identified consistent patterns of nucleotide substitution mutation associated with WDPM. Notably, we found that mutational signature 24 is significantly operative in all five WDPM cases (**Fig. 2B**). In addition to this, mutational signature 21, and 28 were also observed in the WDPM cases.

We identified 461 unique non-silent mutations across five WDPM samples affecting 297 unique protein coding genes (**Supplementary Table 3**). Patient WDPM-04 had the highest mutation burden and WDPM-01 had the least. Two genes - *FBXO10* and *SH2D2A*, were mutated in all five WDPM cases again displaying consistent mutational patterns (**Fig. 2C**). Missense mutation *EHD1*^{D147A} in the dynamin protein domain was found in four cases (**Fig. 2C-D**). The variant allele frequency (VAF) of *EHD1* ranged from 29-43% indicating its likely clonal origin (given that the tumor cellularity of the WDPM tissues were estimated to be about 50%) (**Supplementary Figure 1**). Notably, we identified missense mutation in DNA-damage response gene *ATM* in four cases (**Fig. 2C and 2E**). All four cases harbored

ATM^{K2303R} located in the FRAP-ATM-TRRAP (FAT) domain in ATM protein. The VAF of *ATM* also ranged from 25-30% indicating its likely clonal origin (**Supplementary Figure 1**). The gene encoding cadherin 5 (*CDH5*) harbored *CDH5*^{D714E} mutations in its C-terminus cadherin protein domain in four cases (**Fig. 2C and 2F**). The VAF of *CDH5* also ranged from 26-38% indicating its likely clonal origin (**Supplementary Figure 1**). We also identified missense mutation *FBXO10*^{C42F} in four cases and *FBXO10*^{C26F} in one case (**Fig. 2C and 2G**). Both mutation variants of *FBXO10* were present in F-box like protein domain. The VAF of *FBXO10* also ranged from 24-37% indicating its likely clonal origin (**Supplementary Figure 1**). Similarly, we identified missense mutation *SH2D2A*^{G155V} in four cases and *SH2D2A*^{G155D} in one case (**Fig. 2C and 2H**). These variants were located in SH2 protein domain. The VAF of *SH2D2A* in WDPM-04 was 69% indicating the mutation to be clonal. The VAF of *SH2D2A* in rest of the four WDPM ranged from 37-47% (**Supplementary Figure 1**). Furthermore, we also identified mutations in *MAGED1* and *TP73* each in four WDPM cases (**Fig. 2C**).

Copy Number Aberration landscape of WDPM

The aggregate copy number aberration (CNA) profile of WDPM is shown in **Supplementary Figure 2**. We observed 278 CNA events across all samples (**Supplementary Table 4**). The CNA resulted in alterations of about 4-14% of the protein-coding genomes in WDPM. Patient WDPM-02 had a high copy-number burden and WDPM-03 had the least copy-number burden (**Supplementary Figure 2**). Overall, copy number profiles of WDPM did not show many alterations (**Supplementary Figure 3**). Notably, we found copy number gain of *SETDB2* and *LAST2*, and copy number loss of *SMARCA4* and *TRAF7* in WDPM-02. We also found copy-number loss of cancer genes such as *CCNE1*, *MAF*, *MAFB*, *MYC*, *ZNF479*, *MGMT* and copy number gain of *FOXA2*, *CDH10*, *GPC5* in at least two WDPM cases.

Signaling pathways dysregulated in WDPM

To identify signaling pathways dysregulated by mutated genes in WDPM, we performed pathway enrichment analysis using KEGG[18] pathway database (see Methods section). Our analysis revealed that the WDPM mutations target different signaling pathways often dysregulated in cancer (**Fig. 3 and Supplementary Table 5**) such as Pathways in Cancer, Focal Adhesion, VEGF Signaling, JAK-STAT Signaling, WNT Signaling, P53 Signaling, Apoptosis, etc. We found *CDH5* mutations target Cell Adhesion and Leukocyte Migration pathway; *EHD1* mutations target Endocytosis; *SH2D2A* mutation target VEGF Signaling pathway; *ATM* mutation target Apoptosis and P53 Signaling pathways; and

TP73 target Neurotrophin Signaling and P53 Signaling pathways. This indicates that the mutations identified in WDPM cases might be relevant to pathogenesis of WDPM.

WDPM is genetically distinct from malignant mesothelioma

Next, we compared the genomic profiles of WDPM with those of malignant peritoneal mesothelioma. For this, we leveraged the DNA sequencing data from two recently published peritoneal mesothelioma patient cohorts[6,20]. We first assessed the pattern of mutations in WDPM and peritoneal mesothelioma cases. Intriguingly, we observed that WDPM has a strong enrichment of C>A transversion substitution mutation (**Fig. 2A-B**), whereas, peritoneal mesothelioma has strong enrichment of C>T transition substitution mutation (**Supplementary Figure 4**). This mutational pattern in WDPM is different from those reported in pleural[4,5] or peritoneal[6] mesotheliomas.

Notably, we found WDPM specific mutations in *EHD1*, *FBXO10*, *CHD5*, *MAGED1*, *ATM*, and *TP73* genes that were absent in peritoneal mesothelioma (**Fig. 4A**). Although, mutations in *EHD1* and *ATM* genes were each observed in peritoneal mesothelioma, we did not find the WDPM specific *EHD1*^{D147A}, *EHD1*^{A465D}, and *ATM*^{K2303R} mutations in these cases. Interestingly, we did not find any mutations in *BAP1*, *SETD2*, *TP53*, *NF2*, *CDKN2A*, and *LAST1/2* frequently observed in malignant mesotheliomas (**Fig. 4A**). We also did not find mutations in *TRAF7* or *CDC42* in WDPM, however, *TRAF7* mutations were observed in several peritoneal mesothelioma cases. Furthermore, we evaluated the differences in copy number status of genes between WDPM and peritoneal mesothelioma. We did not find any copy-number loss in genes characteristics of malignant mesotheliomas such as *BAP1*, *SETD2*, *PBRM1*, *SMARCC1*, *CDKN2A/B*, *LATS1/2* and *NF2* (**Fig. 4B**). *TRAF* copy-number loss was observed in one WDPM case, whereas, several peritoneal mesothelioma cases harbored *TRAF7* copy-number alteration.

Discussion

In this study, we have investigated the genomic alterations found in a cohort of five WDPM. The tumors analyzed here are clinically typical of the setting in which WDPM is most commonly found; i.e., as an incidental lesion discovered during surgery for another process, and all of the lesions were morphologically characteristic WDPM.

Overall, our results suggest that WDPM are distinctive lesion with their own set of genomic alterations and are genetically quite different from both peritoneal and pleural mesotheliomas. Indeed, our most important finding is the lack of alterations involving *BAP1*, *SETD2*, *NF2*, *CDKN2A*, *PBRM1*, and *SMARCC1* genes consistently mutated or deleted in malignant mesotheliomas.

We found consistent mutation patterns in five WDPMs with strong enrichment of C>A transversion substitution mutation and COSMIC mutational signature 24. The WDPMs harbored distinct mutations in *EHD1*, *FBXO10*, *CHD5*, *MAGED1*, *ATM*, and *TP73* genes either in all five or at least four out of five WDPM cases. The COSMIC mutational signature 24 has been shown to be commonly found in certain liver cancers with exposure to carcinogen such as aflatoxin[22]. However, these WDPMs were incidental findings during surgery and any prior exposure to carcinogens (either aflatoxin or asbestos) is extremely unlikely. Mutations and copy-number changes in *CDH5* has been previously reported in mesotheliomas[23,24], but are uncommon events and were not present in any of our reference mesothelioma datasets (**Fig. 3**). CHD5 is known to promote intravasation and stimulates TGF-β driven epithelial–mesenchymal transition (EMT)[25]. *EHD1* regulates endocytic recycling process. *EHD1* is known to play a key role in transportation of receptors from endosomes into the endocytic recycling compartment (ERC) and from the ERC to the plasma membrane[26]. Moreover, *EHD1* has been associated with cell proliferation, apoptosis, metastasis, and drug resistance in breast and non-small cell lung cancer (NSCLC)[27], but has not been reported to be abnormal in malignant mesotheliomas. *FBXO10* binds to the anti-apoptotic oncoprotein BCL-2 and promotes its degradation, thereby initiating cell death in lymphomas[28]. *SH2D2A* is known to be involved in T-cell activation[29]. Mutations in *FBXO10*, *SH2D2A*, and *TP73* has not been reported in any malignant mesotheliomas.

Our study confirms lack of copy-number alterations in *BAP1*, *SETD2*, *PBRM1*, *SMARCC1*, *CDKN2A/B*, *LATS1/2*, and *NF2*. Copy-number loss of *BAP1*, *SETD2*, *PBRM1*, and *SMARCC1* is often observed in peritoneal mesothelioma[6,30]. Copy-number loss of *BAP1*, *CDKN2A/B*, *LAST1/2*, and *NF2* is frequently found in pleural mesothelioma[4,5].

What is surprising in our results is the absence of the *TRAF7* and *CDC42* alterations reported by Yu *et al.*[7] and Stevers *et al.*[11] in WDPM and by the same group in adenomatoid tumors[31]. Alterations in *TRAF7* has also been reported in malignant mesotheliomas[4,20,32]. However, this does not appear to be a case of tumor misclassification, since the lesion illustrated by Stevers *et al.* is a very typical WDPM and is identical to the tumors analyzed here. The lesions analyzed by Stevers *et al.* were also all incidental findings and 8/10 were solitary, as were ours, and the lesions for which they had follow up did not behave in a malignant fashion. This likely indicates genomic heterogeneity in WDPM and warrants further investigation in large patient cohort settings.

In summary, we have shown that WDPMs are genetically distinct from malignant mesotheliomas and in our hands have a characteristic pattern of C>A transversion substitution mutations; *EHD1*, *FBXO10*, *CHD5*, *MAGED1*, *ATM*, and *TP73* missense mutations; as well as enrichment of COSMIC mutation signature 24. Taken in conjunction with the data from Stevers *et al.*, these finding further reinforce the idea that WDPM should not be treated in the same fashion as malignant mesotheliomas.

Acknowledgments

This study is funded by: BC Cancer Foundation, Mitacs, Canadian Institutes of Health Research (CIHR), and Terry Fox Research Institute (C.C.C. and Y.Z.W.). R.S. and N.N. are supported by Mitacs Accelerate Awards.

Conflict of Interest

The authors declare that they have no conflict of interest.

References

1. Daya D, McCaughey WT. Well-differentiated papillary mesothelioma of the peritoneum. A clinicopathologic study of 22 cases. *Cancer* 1990;65:292–6. Available at: http://www.ncbi.nlm.nih.gov/pubmed/2295052.

2. Butnor KJ, Sporn TA, Hammar SP, et al. Well-differentiated papillary mesothelioma. *Am. J. Surg. Pathol.* 2001;25:1304–9. doi:10.1097/PAS.0000000000000200.

3. Deraco M, Nizri E, Glehen O, et al. Well differentiated papillary peritoneal mesothelioma treated by cytoreduction and hyperthermic intraperitoneal chemotherapy-the experience of the PSOGI registry. *Eur. J. Surg. Oncol.* 2019;45:371–375. doi:10.1016/j.ejso.2018.10.065.

4. Bueno R, Stawiski EW, Goldstein LD, et al. Comprehensive genomic analysis of malignant pleural mesothelioma identifies recurrent mutations, gene fusions and splicing alterations. *Nat. Genet.* 2016;48:407–16. doi:10.1038/ng.3520.

5. Hmeljak J, Sanchez-Vega F, Hoadley KA, et al. Integrative Molecular Characterization of Malignant Pleural Mesothelioma. *Cancer Discov.* 2018;8:1548–1565. doi:10.1158/2159-8290.CD-18-0804.

6. Shrestha R, Nabavi N, Lin Y-Y, et al. BAP1 haploinsufficiency predicts a distinct immunogenic class of malignant peritoneal mesothelioma. *Genome Med.* 2019;11:8. doi:10.1186/s13073-019-0620-3.

7. Yu W, Chan-On W, Teo M, et al. First somatic mutation of E2F1 in a critical DNA binding residue discovered in well-differentiated papillary mesothelioma of the peritoneum. *Genome Biol.* 2011;12:R96. doi:10.1186/gb-2011-12-9-r96.

8. Nemoto H, Tate G, Kishimoto K, et al. Heterozygous loss of NF2 is an early molecular alteration in well-differentiated papillary mesothelioma of the peritoneum. *Cancer Genet.* 2012;205:594–598. doi:10.1016/j.cancergen.2012.08.005.

9. Ribeiro C, Campelos S, Moura CS, et al. Well-differentiated papillary mesothelioma: Clustering in a Portuguese family with a germline BAP1 mutation. *Ann. Oncol.* 2013;24:2147–2150. doi:10.1093/annonc/mdt135.

10. Lee HE, Molina JR, Sukov WR, et al. BAP1 loss is unusual in well-differentiated papillary mesothelioma and may predict development of malignant mesothelioma. *Hum. Pathol.* 2018;79:168–176. doi:10.1016/j.humpath.2018.05.001.

11. Stevers M, Rabban JT, Garg K, et al. Well-differentiated papillary mesothelioma of the peritoneum is genetically defined by mutually exclusive mutations in TRAF7 and CDC42. *Mod. Pathol.* 2019;32:88–99. doi:10.1038/s41379-018-0127-2.

12. Wang K, Li M, Hakonarson H. ANNOVAR: functional annotation of genetic variants from high-throughput sequencing data. *Nucleic Acids Res.* 2010;38:e164. doi:10.1093/nar/gkq603.

13. Thorvaldsdóttir H, Robinson JT, Mesirov JP. Integrative Genomics Viewer (IGV): high-performance genomics data visualization and exploration. *Brief. Bioinform.* 2013;14:178–92. doi:10.1093/bib/bbs017.

14. Mayakonda A, Lin D-C, Assenov Y, et al. Maftools: efficient and comprehensive analysis of somatic variants in cancer. *Genome Res.* 2018;28:1747–1756. doi:10.1101/gr.239244.118.

15. Mermel CH, Schumacher SE, Hill B, et al. GISTIC2.0 facilitates sensitive and confident localization of the targets of focal somatic copy-number alteration in human cancers. *Genome Biol.* 2011;12:R41. doi:10.1186/gb-2011-12-4-r41.

16. Rosenthal R, McGranahan N, Herrero J, et al. DeconstructSigs: delineating mutational processes in single tumors distinguishes DNA repair deficiencies and patterns of carcinoma evolution. *Genome Biol.* 2016;17:31. doi:10.1186/s13059-016-0893-4.

17. Alexandrov LB, Jones PH, Wedge DC, et al. Clock-like mutational processes in human somatic cells. *Nat. Genet.* 2015;47:1402–1407. doi:10.1038/ng.3441.

18. Kanehisa M, Sato Y, Furumichi M, et al. New approach for understanding genome variations in KEGG. *Nucleic Acids Res.* 2019;47:D590–D595. doi:10.1093/nar/gky962.

19. Subramanian A, Tamayo P, Mootha VK, et al. Gene set enrichment analysis: a knowledge-based approach for interpreting genome-wide expression profiles. *Proc. Natl. Acad. Sci. U. S. A.* 2005;102:15545–50. doi:10.1073/pnas.0506580102.

20. AACR Project GENIE Consortium. AACR Project GENIE: Powering Precision Medicine

through an International Consortium. *Cancer Discov.* 2017;7:818–831. doi:10.1158/2159-8290.CD-17-0151.

21. Travis WD, Brambilla E, Müller-Hermelink HK, et al. *Pathology and Genetics of Tumours of the Lung, Pleura, Thymus and Heart*. (Travis WD, Brambilla E, Müller-Hermelink HK, et al., eds.). Lyon, France: WHO Press; 2004.

22. Huang MN, Yu W, Teoh WW, et al. Genome-scale mutational signatures of aflatoxin in cells, mice, and human tumors. *Genome Res.* 2017;27:1475–1486. doi:10.1101/gr.220038.116.

23. Bott M, Brevet M, Taylor BS, et al. The nuclear deubiquitinase BAP1 is commonly inactivated by somatic mutations and 3p21.1 losses in malignant pleural mesothelioma. *Nat. Genet.* 2011;43:668–672. doi:10.1038/ng.855.

24. Chirac P, Maillet D, Leprêtre F, et al. Genomic copy number alterations in 33 malignant peritoneal mesothelioma analyzed by comparative genomic hybridization array. *Hum. Pathol.* 2016;55:72–82. doi:10.1016/j.humpath.2016.04.015.

25. van Roy F. Beyond E-cadherin: roles of other cadherin superfamily members in cancer. *Nat. Rev. Cancer* 2014;14:121–34. doi:10.1038/nrc3647.

26. Grant BD, Donaldson JG. Pathways and mechanisms of endocytic recycling. *Nat. Rev. Mol. Cell Biol.* 2009;10:597–608. doi:10.1038/nrm2755.

27. Wang X, Yin H, Zhang H, et al. NF-κB-driven improvement of EHD1 contributes to erlotinib resistance in EGFR-mutant lung cancers. *Cell Death Dis.* 2018;9:418. doi:10.1038/s41419-018-0447-7.

28. Chiorazzi M, Rui L, Yang Y, et al. Related F-box proteins control cell death in Caenorhabditis elegans and human lymphoma. *Proc. Natl. Acad. Sci. U. S. A.* 2013;110:3943–8. doi:10.1073/pnas.1217271110.

29. Acuto O, Bartolo V Di, Michel F. Tailoring T-cell receptor signals by proximal negative feedback mechanisms. *Nat. Rev. Immunol.* 2008;8:699–712. doi:10.1038/nri2397.

30. Yoshikawa Y, Emi M, Hashimoto-Tamaoki T, et al. High-density array-CGH with targeted NGS unmask multiple noncontiguous minute deletions on chromosome 3p21 in mesothelioma. *Proc.*

Natl. Acad. Sci. U. S. A. 2016;113:13432–13437. doi:10.1073/pnas.1612074113.

31. Goode B, Joseph NM, Stevers M, et al. Adenomatoid tumors of the male and female genital tract are defined by TRAF7 mutations that drive aberrant NF-kB pathway activation. *Mod. Pathol.* 2018;31:660–673. doi:10.1038/modpathol.2017.153.

32. Sneddon S, Dick I, Lee YCG, et al. Malignant cells from pleural fluids in malignant mesothelioma patients reveal novel mutations. *Lung Cancer* 2018;119:64–70. doi:10.1016/j.lungcan.2018.03.009.

Figures

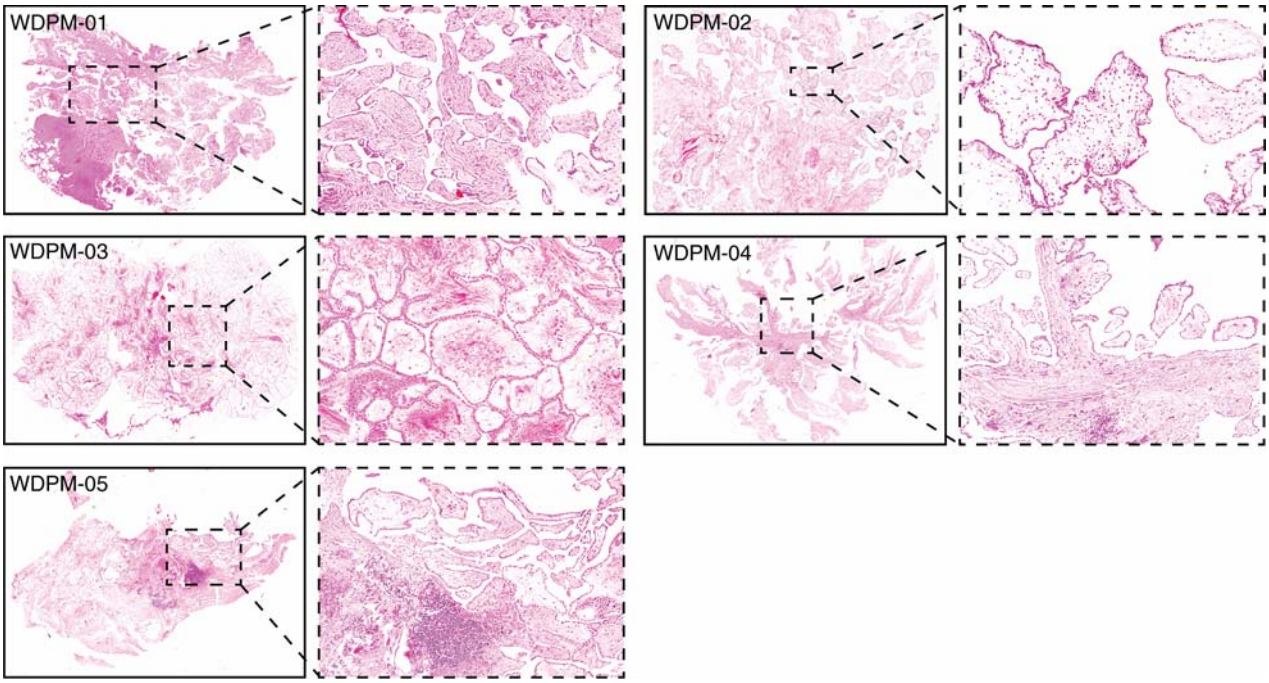

Figure 1. Histopathology of five WDPM cases used for the study. Microphotographs of histological features of WDPM stained using Haematoxylin and eosin (H&E). The panel under the dotted box represents the magnified section of the photomicrographs at ×20.

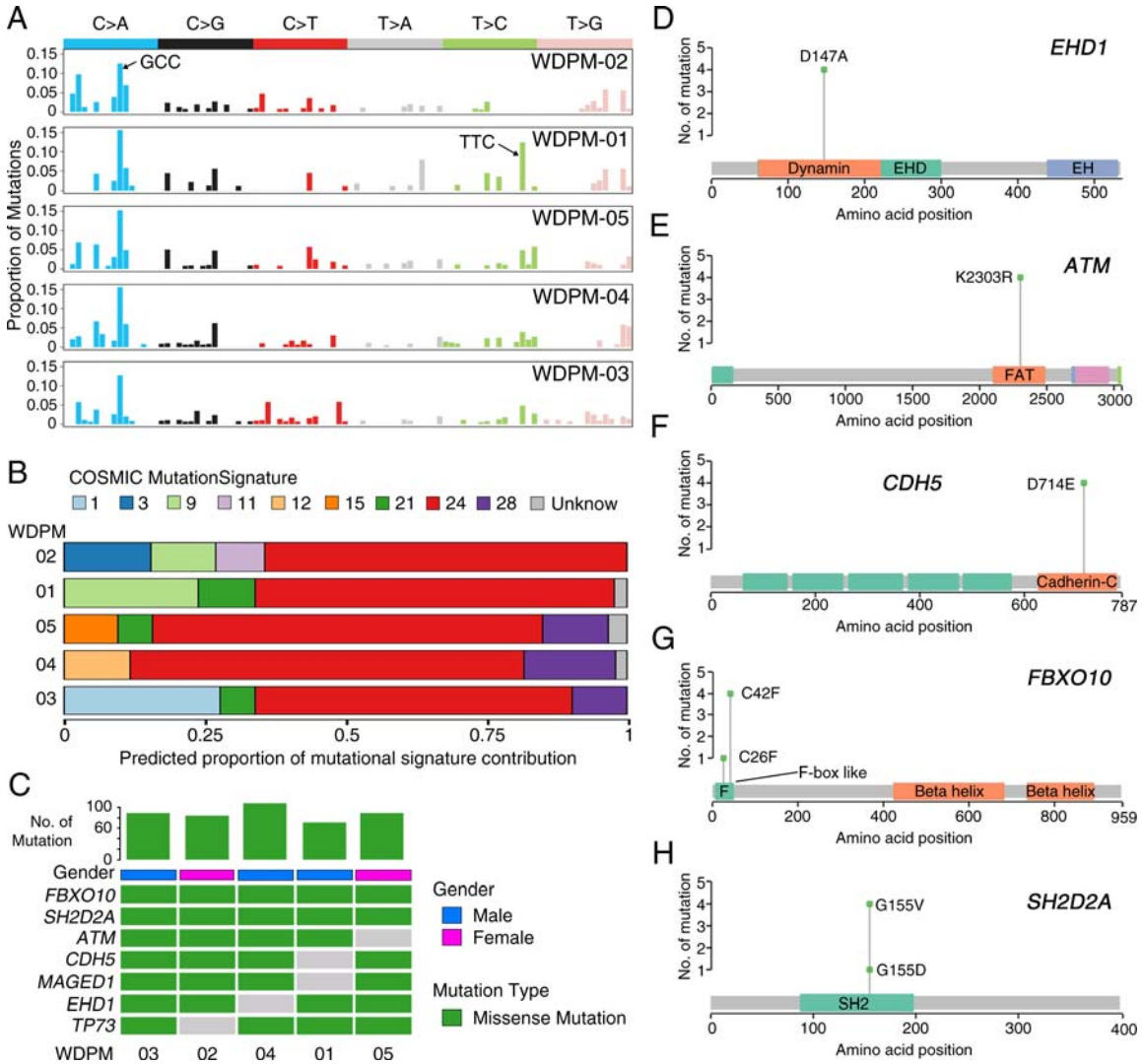

Figure 2. Landscape of somatic mutations in WDPM. (A) Mutational signature present in WDPM. (B) Proportional contribution of different COSMIC mutational signature per sample. (C) Somatic mutation status in WDPM. Top seven most recurrent mutations are represented in the figure. The bar plot on the top panel represents the total number of mutations detected in the respective WDPM. (D-H) Plots showing mutation distribution and the protein domains for the corresponding mutated protein.

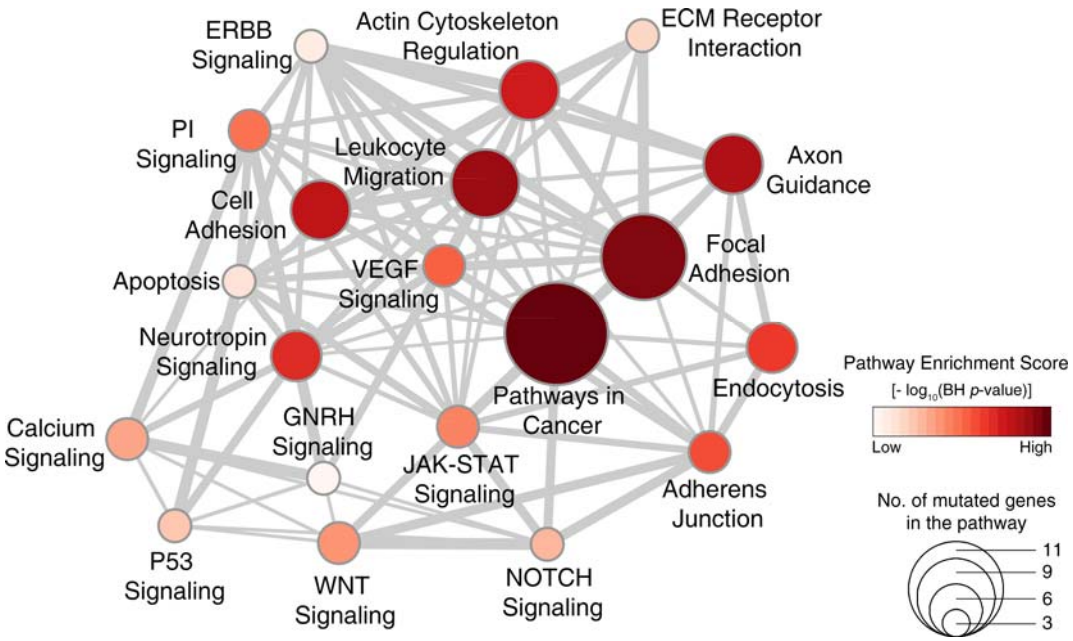

Figure 3. Signaling pathways dysregulated in WDPM. We performed pathway enrichment analysis using genes mutated in WDPM cases against the signaling pathways in the KEGG pathway database. The figure shows top-20 pathways enriched with mutated genes in WDPM. Each circle represents a pathway, its size indicates the number of mutated genes targeting the pathway, and its color indicates the Pathway Enrichment Score. The thickness of edges connecting two circles (pathways) is proportional to the number of mutated genes common between the two pathways. PI Signaling: Phosphatidylinositol Signaling Pathway.

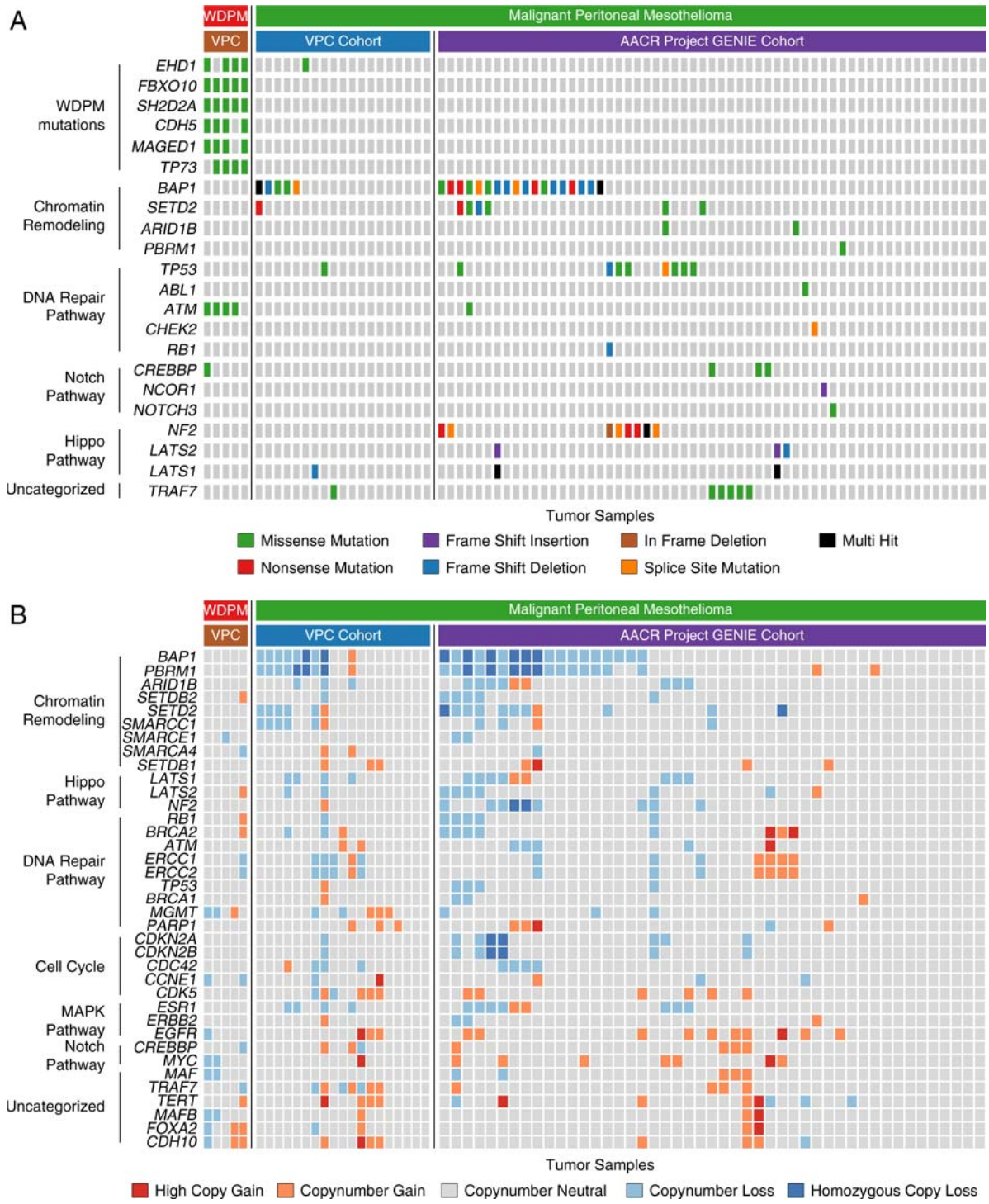

Figure 4. Genomic alterations in WDPM and Peritoneal Mesothelioma. We compared the genomic alteration profile of the WDPM cases to the peritoneal mesothelioma patient cohorts from two recently published studies, VPC cohort[6] and AACR Project GENIE Cohort[20]. (A) Oncoplot showing differences in somatic mutation pattern between WDPM and peritoneal mesothelioma. Each column in the figure

represent an individual cancer sample. (B) Oncoplot showing the copy-number aberration status of WDPM and peritoneal mesothelioma. Each column in the figure represent an individual cancer sample.